

# PriSampler: Mitigating Property Inference of Diffusion Models

Hailong Hu

*SnT, University of Luxembourg*

Jun Pang

*FSTM & SnT, University of Luxembourg*

## Abstract

Diffusion models have been remarkably successful in data synthesis. Such successes have also driven diffusion models to apply to sensitive data, such as human face data, but this might bring about severe privacy concerns. In this work, we systematically present the first privacy study about property inference attacks against diffusion models, in which adversaries aim to extract sensitive global properties of the training set from a diffusion model, such as the proportion of the training data for certain sensitive properties. Specifically, we consider the most practical attack scenario: adversaries are only allowed to obtain synthetic data. Under this realistic scenario, we evaluate the property inference attacks on different types of samplers and diffusion models. A broad range of evaluations shows that various diffusion models and their samplers are all vulnerable to property inference attacks. Furthermore, one case study on off-the-shelf pre-trained diffusion models also demonstrates the effectiveness of the attack in practice. Finally, we propose a new model-agnostic plug-in method PriSampler to mitigate the property inference of diffusion models. PriSampler can be directly applied to well-trained diffusion models and support both stochastic and deterministic sampling. Extensive experiments illustrate the effectiveness of our defense and it makes adversaries infer the proportion of properties as close as random guesses. PriSampler also shows its significantly superior performance to diffusion models trained with differential privacy on both model utility and defense performance.

## 1 Introduction

Diffusion models [38], as an emerging class of generative models, have gained widespread adoption in a large number of application areas, such as image synthesis [14, 18, 40, 41], text-to-image generation [30, 32], and even text generation [12, 23], and video creation [16, 22]. However, when sensitive and private datasets, such as human face data, are applied to train diffusion models, it might cause various privacy breaches.

In general, there are two main types of attacks in relation to privacy: membership inference attacks [37] and property inference attacks [3]. Membership inference attacks aim to infer whether one sample was used for training a machine learning model. Recent works have already demonstrated that diffusion models are vulnerable to membership inference attacks and can memorize some training samples [4, 9, 17, 28, 44, 49]. Unlike membership inference attacks focusing on revealing the privacy of the individual samples of a training dataset, the goal of property inference attacks is to infer global properties of the whole training set of a machine learning model, such as inferring the proportion of certain sensitive properties of a training set. Although a considerable body of works has studied property inference attacks in classification models, such as support vector machines [3], fully-connected neural networks [11], convolution neural networks [5, 27, 42], and generative adversarial networks [48], even graph neural networks [47], property inference of diffusion models has not been explored to date. Considering the popularity of diffusion models and the fact that diffusion models are now the dominant paradigm in deep generative modeling [6, 20, 45], it is paramount to systematically study the property inference risks of diffusion models.

**Attacks.** In this work, we investigate the privacy risks of diffusion models through the lens of property inference attacks. Our threat model assumes that adversaries can only have access to generated samples from a diffusion model. Based on generated samples, our property inference attack aims to estimate the proportion of various properties of a diffusion model by a property classifier (see Section 4.2). We explore four different types of diffusion models, including the discrete variance preserving (VP) model — DDPM [14], the discrete variance exploding preserving (VE) model — SMLD [40], the continuous VP model — VPSDE [41] and the continuous VE model — VESDE [41]. Unlike other generative models, such as generative adversarial networks [13] or variational autoencoder [21], for a trained diffusion model, there are different sampling methods to generate samples, in which these methods aim to improve the quality of gener-

ated samples or sampling speed during the sampling process. Therefore, we study three samplers over two different types of sampling mechanisms, including stochastic sampling — PC sampler [41] and deterministic sampling — the black-box ODE sampler [8] and the DPM sampler [26].

Our comprehensive experiments on the human face dataset CelebA [25] demonstrate that state-of-the-art diffusion models and their samplers are vulnerable to property inference attacks (see Section 4.4). Adversaries can precisely infer the proportion of sensitive properties with 0% absolute difference in the best case and below 7% absolute difference in the worst case, where the absolute difference refers to the difference between the inferred proportion and the real proportion. We further explore the performance of property inference in terms of different properties, the number of generated samples, and model performance.

**Case study.** We conduct one case study where target models are from off-the-shelf diffusion models EDM [18] trained on a human face dataset FFHQ [19]. We again see similar excellent attack performance on EDM models. Our attack results show that at least 0.23% absolute difference and at most 3.97% absolute difference can be achieved on inferring the property Young. For the property gender, the absolute difference does not exceed 1.23%, which indicates the inferred proportion is highly close to the real proportion (see Section 5).

**Defenses.** To defend against property inference attacks, we propose a property aware sampling method — PriSampler, which manipulates diffusion models in the sampling process to conceal the real proportion of sensitive properties. More specifically, our defense method first finds the hyperplanes of properties in the diffusion models, and the learned hyperplanes are utilized to guide one sampler to synthesize samples in this property space (see Figure 7). We show the effectiveness of our defense method PriSampler on different types of samplers, diffusion models, more properties, and the number of generated samples and different diffusion steps (see Section 6.5). We also compare PriSampler with differentially private diffusion models (DDPMs) [7], and evaluations show that PriSampler is superior to DDPMs on model utility and defense performance (see Section 6.6). More importantly, PriSampler does not require re-training a diffusion model.

**Contributions.** Our contributions in this paper are threefold.

- (1) We perform the first study of property inference attacks against diffusion models under the most practical attack scenario, showing that diffusion models and their samplers are vulnerable to property inference attacks.
- (2) We conduct one case study to demonstrate privacy risks of property inference of diffusion models in practice.
- (3) We propose the first model-agnostic and plug-in defense — PriSampler to mitigate property inference attacks against diffusion models, illustrating that our method achieves state-of-the-art performance in both model utility and defense performance.

## 2 Background

This section presents some background information on different diffusion models and different sampling mechanisms.

### 2.1 Diffusion Models

A diffusion model is a generative model, and it aims to learn the distribution  $p_{data}$  of a training set and generate new unseen data samples. In general, it consists of two processes: a forward process and a reverse process. In the forward process, it adds different levels of noise  $0 = \sigma_0 < \sigma_1 < \dots < \sigma_T = \sigma_{max}$  into training data, in order to transform a training data’s distribution into a Gaussian distribution within  $T$  time steps. In the reverse process, it randomly samples a noise image from the Gaussian distribution and gradually denoises it into an image. In the following, we introduce three fundamental types of diffusion models.

**DDPM.** The denoising diffusion probabilistic model (DDPM) is proposed by Ho et al. [14]. In the forward process, a sample at the  $t$  time step is perturbed by:  $x_t \leftarrow \sqrt{\alpha_t}x_0 + \sqrt{1 - \alpha_t}\epsilon$ , where  $\epsilon \sim \mathcal{N}(0, I)$ ,  $x_0 \sim p_{data}$ , and  $\alpha_t \in [0, 1]$  is a variance schedule to control the magnitude of noise in each time step.  $\alpha_0 = 1$  means that an image at  $t = 0$  time step is not perturbed and  $\alpha_T = 0$  indicates that the perturbed image at  $t = T$  time step becomes pure Gaussian noise. In the reverse process, a noise image from  $\mathcal{N}(0, I)$  is step by step denoised and eventually recovers a noise-free image, and during the process a neural network  $\epsilon_\theta(x_t, t)$  is trained to predict noise by minimizing the following loss:

$$L(\theta) = \mathbb{E}_{t \sim [1, T], x \sim p_{data}, \epsilon \sim \mathcal{N}(0, I)} [\|\epsilon - \epsilon_\theta(\sqrt{\alpha_t}x + \sqrt{1 - \alpha_t}\epsilon, t)\|^2]. \quad (1)$$

**SMLD.** The score matching with Langevin dynamics (SMLD) is proposed by Song et. al [40]. In the forward process, a perturbed sample at the  $t$  time step is obtained by:  $x_t \leftarrow x_0 + \sigma_t\epsilon$ , where  $\sigma_t$  is the noise schedule to control the magnitude of noise. In the reverse process, a neural network  $s_\theta(x_t, \sigma_t)$  is trained to predict *score*. The *score* refers to the gradient of the log probability density with respect to data, i.e.  $\nabla_x \log p(x)$ . SMLD minimizes the following loss:

$$L_\theta = \mathbb{E}_{t \sim [1, T], x \sim p_{data}, x_t \sim q(x_t|x)} [\lambda(\sigma_t) \|s_\theta(x_t, \sigma_t) - \nabla_{x_t} \log q(x_t|x)\|^2], \quad (2)$$

where  $\lambda(\sigma_t)$  is a coefficient function and  $\nabla_{x_t} \log q(x_t|x) = -\frac{x_t - x}{\sigma_t^2}$ .

**SSDE.** The score-based stochastic differential equation (SSDE) proposed by Song et. al [41] presents a general and unified framework for generative modeling. The process of a diffusion model is described as a stochastic differential equation. Specifically, SSDE defines the forward process as:  $dx = f(x, t)dt + g(t)dw$ , where  $f(x, t)$ ,  $g(t)$  and  $dw$  are the drift coefficient, the diffusion coefficient and a standard Wiener process, respectively. In

the reverse process, it can be expressed by a reverse-time SDE:  $dx = [f(x, t) - g(t)^2 \nabla_x \log q_t(x)]dt + g(t)d\bar{w}$ , where  $\bar{w}$  is a standard Wiener process in the reverse time. A neural network is used for predicting *score* by minimizing the loss:

$$L_\theta = \mathbb{E}_{t \in \mathcal{U}(0, T), x \sim p_{data}, x_t \sim q(x_t|x)} [\lambda(t) \|s_\theta(x_t, t) - \nabla_{x_t} \log q(x_t|x)\|^2]. \quad (3)$$

Different coefficients, i.e.  $f(x, t)$  and  $g(t)$ , correspond to different types of SSDE, and in their work, two types of SSDE are proposed: variance preserving (VP) and variance exploding (VE). We call their corresponding models as VPSDE and VESDE and they are continuous diffusion models. Furthermore, under this framework, DDPM and SMLD can be considered discrete VP and VE, respectively. In this work, we will systematically study these four types of diffusion models: DDPM, SMLD, VPSDE, and VESDE.

## 2.2 Samplers

After the training of a diffusion model finishes, we can use different samplers to synthesize new data. Based on the unified framework of SSDE, there are two types of sampling: stochastic sampling and deterministic sampling.

**Stochastic sampling.** Because a diffusion model can be described as a stochastic differential equation (SDE), we can generate a new sample by solving the corresponding reverse-time SDE [2]. Existing general-purpose numerical solvers, such as Euler-Maruyama and stochastic Runge-Kutta methods [31], can be used for solving the SDE. Song et. al [41] propose Predictor-Corrector methods to further improve the sampling quality by utilizing the score-based model. In this work, we call it as PC sampler.

**Deterministic sampling.** In addition to solving a reverse-time SDE, Song et. al [41] find that a reverse-time SDE also corresponds to a probability flow ordinary differential equation (ODE) in which they have the same marginal probability densities. It indicates that we can generate a new sample by solving a probability flow ODE. Existing black-box ODE solver [8] can be used to generate samples. In this work, we call it as ODE sampler.

In addition to directly using a black-box ODE solver, there are many works about designing efficient samplers based on solving the probability flow ODE [24, 26, 46]. For example, DPM [26] analyzes the ODE consisting of a linear function of the data variable and a nonlinear function parametrized by neural networks. By deriving an exact formulation for the linear part, DPM can improve the quality of generated samples and speed up the sampling process. In this work, we call it as DPM sampler. Considering their excellent sampling performance, we will systematically study three samplers from two different sampling mechanisms: PC sampler, ODE sampler, and DPM sampler.

## 3 Motivation and Threat Model

We elaborate on the motivations for our research in Section 3.1 and introduce our threat model in Section 3.2.

### 3.1 Motivation

Diffusion models are widely used in many application domains [20, 45], and one of the primary purposes is to leverage these state-of-the-art diffusion models to generate a diversity of novel images. Beyond these purposes, malicious adversaries might reveal some sensitive information of a training dataset through diffusion models, which usually do not intend to be shared by model owners/providers. For example, a diffusion model trained on a human face dataset is used to generate various different and realistic images. When malicious adversaries obtain this model, instead of only synthesizing novel samples, they could use the shared model to infer sensitive properties, such as the proportion of gender, ethnicity, age, or sentiment. Similarly, even if adversaries only have access to generated samples that are released by model owners, it is possible to infer sensitive information of the training set leaked through generated samples. As a consequence, by successfully inferring sensitive information from a training set, the adversaries can know the proportion of gender or ethnicity of a training set, even the sentiment inclination (negative or positive). These sensitive properties are usually protected and model owners do not intend to share them.

In addition, some properties, such as gender, usually are related to the fairness of a machine learning model. Even though model owners can ensure the fairness of a training set in terms of these properties, a diffusion model might induce unfairness from other factors, such as generative algorithms themselves. Once the adversaries correctly estimate the proportion of these properties and make them public, model owners will face accusations from data regulation institutions.

Therefore, in this work, our goal is to systematically study the feasibility of property inference attacks against diffusion models by considering different state-of-the-art diffusion models and their samplers. Furthermore, based on a wide range of investigations in property inference of diffusion models, we will develop a brand-new and effective defense method to mitigate this type of attack. In the end, we hope our work can elevate the awareness of preventing property inference attacks and encourage privacy-preserving synthetic data release.

### 3.2 Threat Model

Our threat model considers that adversaries only obtain generated samples from a diffusion model. The adversaries do not know the type of diffusion models and the type of their samplers, which is usually the strictest and most practical scenario. Furthermore, we assume that the adversaries have

a shadow dataset which contains properties that adversaries intend to infer.

## 4 Property Inference Attacks

The objective of a property inference attack is to predict the proportion of a property in the training set of a trained diffusion model. This makes adversaries reveal some sensitive information that is not shared by model owners. For instance, in addition to directly utilizing generated samples from a diffusion model, adversaries could also attempt to infer sensitive information disclosed by these generated samples, such as the proportion of the property `male`. It is thus important to investigate the feasibility of property inference attacks against diffusion models. This section starts with problem formulation, we then introduce the attack method and experimental setups. Finally, we present attack results and novel insights.

### 4.1 Problem Formulation

A training dataset  $\mathcal{D}$  has different properties including sensitive ones. Each property is binary and has a real proportion  $p_{s_i}$  in dataset  $\mathcal{D}$ . A diffusion model  $\mathcal{G}$  is trained on the dataset  $\mathcal{D}$ . Now, given  $m$  generated samples  $X$  from the diffusion model  $\mathcal{G}$ , and a property  $s_i$ , adversaries aim to infer the proportion of the property  $\hat{p}_{s_i}$ , in order to make  $\hat{p}_{s_i}$  as close  $p_{s_i}$  as possible. More specifically, the adversaries need to design an attack algorithm  $\mathcal{A}$  to estimate  $\hat{p}_{s_i} = \mathcal{A}(X)$ .

### 4.2 Attack Method

The intuition of our attack is that generated samples have a similar distribution to the training set because a diffusion model learns the distribution of a training set and these generated samples are produced by the diffusion model. Therefore, adversaries might infer the proportion of the (sensitive) properties of the training set from these generated samples. To achieve this, we will first deploy a property classifier to predict the property of generated samples, and then use the average statistics of these generated samples containing the property as the inferred proportions.

Figure 1 illustrates the attack process of the property inference attack. Firstly, a property classifier is trained on a shadow training set. The shadow training set is labeled by the property that adversaries are interested in.  $P$  refers to one sample containing this property while  $\bar{P}$  refers to one sample not containing this property. After finishing the training on the shadow data set, the property classifier takes as input generated data from the diffusion model and outputs binary predictions. Finally, the inferred proportion of one property is estimated by  $\hat{p}_{s_i} = \frac{\sum P}{m}$ . For  $k$  properties, we will train  $k$  property classifiers. Note that, unlike property inference attacks that consider them as a classification problem, i.e. inferring whether a machine learning model contains a

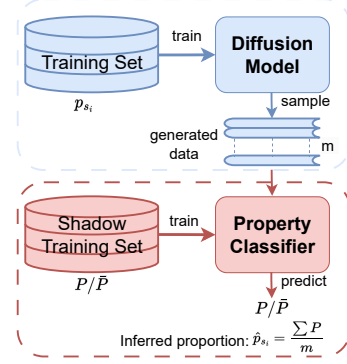


Figure 1: The attack process of the property inference attack.

property [11, 27, 47], here we directly estimate the proportion of a property for diffusion models, which is more precise.

### 4.3 Experimental Setup

**Datasets.** We conduct our experiments on the CelebA dataset which includes 202,599 images of celebrity faces [25]. The reason why we choose this dataset is that it provides a large number of property information. This allows us to more systematically study property inference attacks by considering different proportions of properties. Specifically, the CelebA dataset annotates 40 binary properties for each image. Similar to works [5, 11, 27, 48], we choose four representative properties including `male`, `young`, `smiling`, and `wearing eyeglasses`, which are related to gender, age, sentiment, and personal style. In this work, when it is clear from the context, we will interchangeably use the property name annotated by CelebA, such as `male` and `young`, and the high-level semantic name, such as gender and age.

We design ten datasets with five different proportions of private properties and two different sizes of the training set (i.e.  $10 = 5 \times 2$ ), to investigate the privacy risks of diffusion models. Two sizes of training set include 1k samples and 50k samples, respectively. Five different proportions refer to that male face images account for 10%, 20%, 30%, 40%, and 50% in a dataset, respectively. Different proportions of the `male` property also mean different proportions of the other properties, such as `young` and `smiling`, although the proportions of these properties are not as in sequential order as that of the property `male`. To briefly express its meaning, we mark a dataset as CelebA-size-proportion, such as CelebA-1k-10%. All datasets are resized to  $64 \times 64$ , considering the factors of computation efficiency.

**Target models and samplers.** We use four types of diffusion models: DDPM, SMLD, VPSDE, and VESDE, as the target models, which have been introduced in Section 2. DDPM and VPSDE are trained on 1k samples with five different proportions, while SMLD and VESDE are trained on 50k samples with five different proportions. In total, 20 diffusion models are trained on different training sets. We use open



source codes in this library<sup>1</sup> with their suggested training hyperparameters to train each diffusion model. Specifically, the number of training steps for all models is fixed at 500,000.

We choose three typical samplers: one stochastic sampling — PC sampler, and two deterministic samplings — ODE sampler and DPM sampler. We adopt this library<sup>1</sup> for PC and ODE samplers and this library<sup>2</sup> for the DPM sampler. The recommended sampling hyperparameters in each implementation are adopted. Specifically, the number of sampling steps of DPM is fixed at 40. For the PC sampler, the number of steps of predictor and corrector is 1,000 and 1, respectively. We only study PC samplers for VESDE and SMLD, because they do not support deterministic samplings. However, we investigate all types of samplers for DDPM and VPSDE.

**Attack models.** We use the ResNet-50<sup>3</sup> pre-trained on ImageNet [33] to train a property inference classifier. The shadow training set used for training the classifier is from the remaining samples of the CelebA dataset. In other words, one part of the whole CelebA dataset is used for training diffusion models while the other part, i.e. the shadow training set, is used for training property classifiers. Note that they are disjoint. This is a common practice in the community of privacy in machine learning [5, 11, 48]. In the case study of Section 5, we show that the classifier works just as well for diffusion models trained on different humane face datasets. More specifically, we train classifiers with the stochastic gradient descent optimizer. The learning rate and weight decay of all property classifiers are both 0.01, except for the classifier of the property *young* where both values are set as 0.005. The number of training epochs is set as 5.

**Metrics.** In terms of the performance of diffusion models, we use the widely-adopted Fréchet Inception Distance (FID) metric. A lower FID means that a sampler of a diffusion model can generate more realistic and diverse samples. In this work, by default, we compute an FID with all training samples and 50k generated samples for the ODE and DPM samplers, and 500 generated samples for the PC sampler. This is because the PC sampler requires a much longer time to synthesize data, compared with deterministic ODE and DPM samplers.

In terms of attack performance, our property inference attacks predict a real number, i.e. the proportion of a property. Thus, we show the attack performance by directly presenting the predicted value. In addition, we also report the absolute difference  $\Delta s_i$  between the predicted value and the real value, i.e.  $\Delta s_i = |\hat{p}_{s_i} - p_{s_i}|$ . A smaller absolute difference value means a more precise inference.

## 4.4 Attack Results

In this section, we present the attack results in terms of different samplers, diffusion models, properties, the number of generated samples, and FID values.

**Attack performance on different samplers.** Figure 2 shows attack performance with regard to different samplers over four types of diffusion models. Each type of diffusion model is trained on datasets with different proportions of the sensitive property *male*. Here, the real proportion of the property *male* is set as 10%, 20%, 30%, 40%, and 50%, respectively. An ideal attack means that the inferred proportion is equal to the real proportion. We take it as a reference and it is shown as the grey diagonal line in Figure 2. Overall, all types of samplers cannot defend against the property inference attack. Our inferred proportions are consistently close to the real proportions with the increase in the real proportion of the property *male*. We do not show the attack performance on the ODE sampler and DPM sampler for SMLD and VESDE models, because both samplers do not support these models.

In Table 1, we show the corresponding quantitative attack results. Again, we can observe that the best inference performance can be seen on the PC sampler for the DDPM trained on CelebA-1k-10%, where the absolute difference is 0%. Even in the worst case for adversaries, at most 6.8% absolute difference can be achieved on the PC sampler for the VESDE trained on CelebA-50k-30%. Table 2 summarizes attack performance in terms of different samplers. We can see that our attacks show the best performance in the PC sampler and slightly inferior performance on the ODE sampler. In a nutshell, our attacks can have at most a 2.78% absolute difference among the three types of samplers.

**Attack performance on different diffusion models.** As shown in Figure 2, we present the attack performance on twenty diffusion models encompassing four different types. Each subfigure presents the attack performance of each type of diffusion model. Table 1 shows the corresponding quantitative results of each diffusion model. Overall, all diffusion models are vulnerable to property inference attacks. Although each trained diffusion model can utilize different samplers, we can see that adversaries can still efficiently extract these sensitive information of a training set, regardless of the used samplers. In particular, our attack can achieve almost perfect inference on VPSDE models for all samplers. The reason why the property inference attack is effective on these diffusion models is that all existing samplers mainly focus on improving the quality of generated samples or sampling speed. The other equally important issue, i.e. privacy, is not considered in their design. In Section 6, we will take the first step to provide privacy protection by developing a property aware sampling method for diffusion models.

Table 2 summarizes attack results about different types of diffusion models. We can see our attacks show the best performance on the VPSDE with an average absolute difference

<sup>1</sup>[https://github.com/yang-song/score\\_sde\\_pytorch](https://github.com/yang-song/score_sde_pytorch)

<sup>2</sup><https://github.com/LuChengTHU/dpm-solver>

<sup>3</sup><https://download.pytorch.org/models/resnet50-19c8e357.pth>

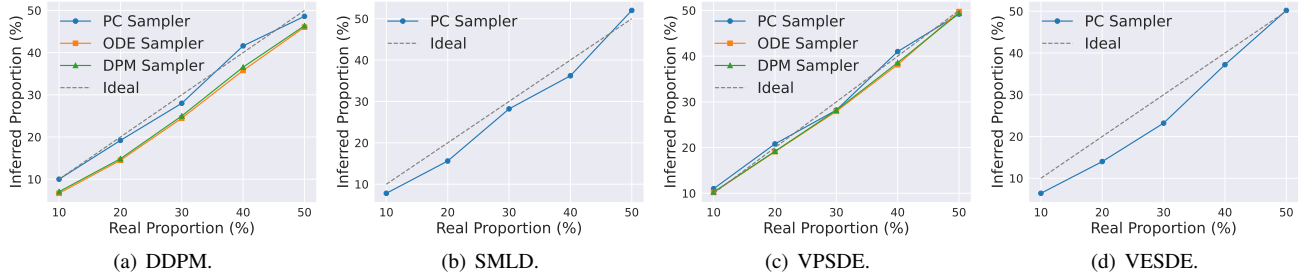


Figure 2: Attack performance on different diffusion models, different samplers, and different proportions of the private property. Here, the sensitive property is male.

Table 1: The qualitative attack results for the sensitive property male. Prop.: proportion. Abs. Diff. : absolute difference.

Model	Real Prop. (%)	Inferred Prop. (%)	Abs. Diff. (%)	FID	Model	Real Prop. (%)	Inferred Prop. (%)	Abs. Diff. (%)	FID	Model	Real Prop. (%)	Inferred Prop. (%)	Abs. Diff. (%)	FID	Model	Real Prop. (%)	Inferred Prop. (%)	Abs. Diff. (%)	FID
PC Sampler					ODE Sampler					DPM Sampler					VESDE				
DDPM	10	10.00	0.00	24.45	SMLD	10	7.80	2.20	23.24	DDPM	10	6.66	3.34	16.80	VPSDE	10	10.19	0.19	5.59
	20	19.20	0.80	24.85		20	15.60	4.40	24.64		20	14.49	5.51	17.12		20	19.11	0.89	5.64
	30	28.00	2.00	25.55		30	28.20	1.80	24.72		30	24.47	5.53	17.41		30	27.93	2.07	5.97
	40	41.60	1.60	26.57		40	36.20	3.80	25.08		40	35.77	4.23	17.61		40	38.14	1.86	5.95
	50	48.60	1.40	28.96		50	52.00	2.00	25.48		50	46.03	3.97	18.46		50	49.75	0.25	6.22
PC Sampler					ODE Sampler					DPM Sampler					VESDE				
VPSDE	10	11.00	1.00	19.22	SMLD	10	6.40	3.60	37.75	DDPM	10	7.05	2.95	22.60	VPSDE	10	10.29	0.29	8.26
	20	20.80	0.80	20.97		20	14.00	6.00	42.08		20	14.85	5.15	23.47		20	19.18	0.82	8.54
	30	28.20	1.80	20.22		30	23.20	6.80	35.94		30	24.99	5.01	23.34		30	28.16	1.84	8.68
	40	41.00	1.00	20.62		40	37.20	2.80	55.89		40	36.56	3.44	23.43		40	38.57	1.43	8.75
	50	49.20	0.80	21.65		50	50.20	0.20	39.31		50	46.37	3.63	24.47		50	49.37	0.63	8.96

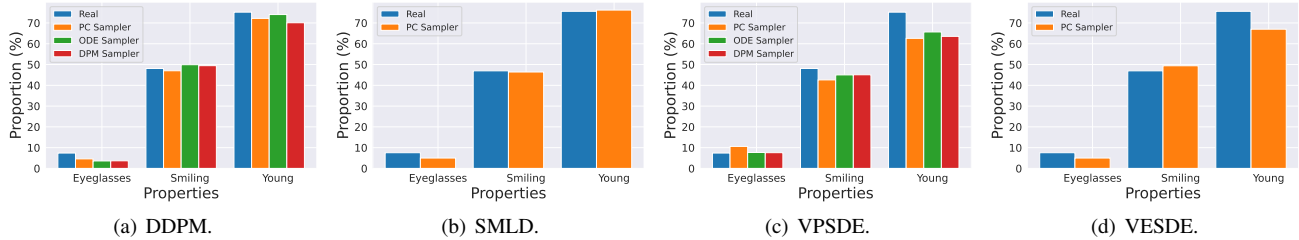


Figure 3: Attack performance on different properties.

Table 2: Summary of attack performances with different types of samplers and diffusion models. Here, we report the average absolute difference (with standard deviation in parentheses) and the best and worst absolute difference.

		Average (%)	Best (%)	Worst (%)
Sampler	PC	2.24 (1.84)	0.00	6.80
	ODE	2.78 (2.02)	0.19	5.53
	DPM	2.52 (1.78)	0.29	5.15
Model	DDPM	3.24 (1.75)	0.00	5.53
	VPSDE	1.04 (0.62)	0.19	2.07
	SMLD	2.84 (1.18)	1.80	4.40
	VESDE	3.88 (2.64)	0.20	6.80

of 1.04%, and show marginally worse performance on the VESDE where the average absolute difference is 3.88%.

**Attack performance on different properties.** In addition to the property male, we also choose other properties. As introduced in Section 4.3, we choose three more properties based on their different proportions in the CelebA dataset. The three properties are eyeglasses, smiling, young and their real proportions are roughly below 10%, close to 50%, and above 70%, respectively. The specific real proportions of these properties are plotted by blue bars in Figure 3. Here, we choose each type of the model with 50% male as the target model. Again, we can observe that our attack still remains effective on inferring the proportions of these properties on all diffusion models and samplers. No matter what the smaller proportion of the property, such as eyeglasses, or the larger proportion of the property, such as young, the inferred proportions are

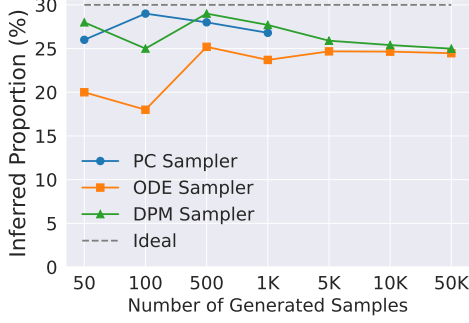


Figure 4: Attack performance with respect to different numbers of generated samples. The target model is DDPM trained on CelebA-1k-30%.

very close to the real proportions.

**Attack performance on different numbers of generated samples.** Figure 4 shows the attack performance on different numbers of generated samples. Here, we choose the DDPM model trained on a dataset that contains 30% `male` training samples, as the target model. We can observe that with the increase in the number of generated samples, the attack performance will gradually become stable. Our attack can be still successful on the PC sampler and DPM sampler even if model owners publish only 50 generated samples, where the absolute difference of both samplers is still below 5%. On the other hand, our attack requires more generated samples for the case of ODE sampler in to achieve a good inference performance but its attack performance shows stable after 500 generated samples.

**Attack performance on different FID values.** Figure 5 shows attack performance in terms of different FID values of target models. Here, we choose the DPM sampler and the VPSDE model trained on CelebA-1k-30%. Furthermore, we choose ten snapshots of VPSDE during the training process. The left axis presents the absolute difference of a target model marked as the blue line, while the right axis shows the FID values of a target model which is marked as the red line. Overall, our attack becomes more accurate with the increase in the performance of target models. Note that a smaller FID means a better utility performance of a target model. This also indicates that pursuing the good utility performance of a diffusion model can lead to more severe privacy risks. Both model utility and privacy risks should be considered when diffusion models involve sensitive data.

**Takeaways.** In summary, (1) both stochastic sampling and deterministic sampling are susceptible to the property inference attack. (2) Different types of diffusion models cannot defend against this attack. (3) No matter how large or small the proportion of certain properties is, our attack can precisely infer them. (4) Inference performance becomes gradually stable after releasing 500 generated samples. (5) The better the utility performance of a diffusion model is, the better the attack performance of property inference.

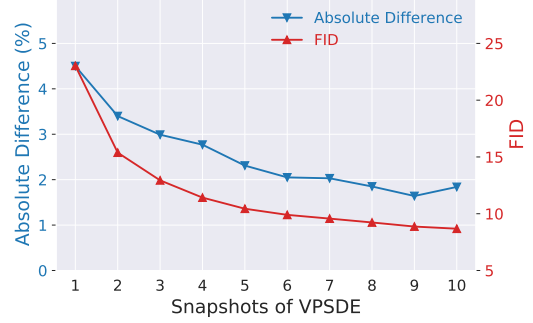


Figure 5: Performance with respect to different FID values. The target model is VPSDE trained on CelebA-1k-30%.

## 5 Case Study: Attacks in Practice

In this section, we further demonstrate the property inference risks in practice through one case study in which we perform property inference attacks against publicly available well-trained diffusion models.

We choose EDM models proposed by Karras et. al [18] as target models. EDM models achieve competitive performance in image synthesis by a design space to decouple complex components. Similar to SSDE introduced in Section 2.1, EDM models include VP and VE formulations, and in this work, we call them VPEDM and VEEDM, respectively. For each model type, they also have two types of sampling methods to synthesize samples: stochastic sampling and deterministic sampling. In our experiments, we conduct property inference attacks on VPEDM and VEEDM. They are both trained by their original authors on the Flickr-Faces-HQ (FFHQ) dataset which contains 70,000 human face images [19]. All samples of the FFHQ dataset used for training have  $64 \times 64$  resolution.

Similarly, we assume that only generated samples can be obtained by adversaries. Because the FFHQ dataset does not annotate the properties of each image, here we use the proportion of the property in the training set inferred by our property inference classifier as the real proportion. Although this might bring some errors due to a lack of human annotation, we report the attack performance by both the inferred proportion and the absolute difference. The absolute difference can eliminate this type of error because it shows attack performance by how close the real and inferred proportions are. In this case study, we directly use the property classifier used in Section 4 to infer the proportion of different properties, which also illustrates the shadow dataset does not have to be from the same dataset of the target models. 50,000 generated samples for all sampling methods and diffusion models are used to perform the property inference. We choose four properties: eyeglasses, smiling, young and male.

**Results.** Figure 6 presents the performance of property inference attacks against EDM models over four properties. Overall, our attack can achieve a rather precise estimation for the proportion of each property. Although the real proportion of these four properties has wide ranges from 29% to 53%,

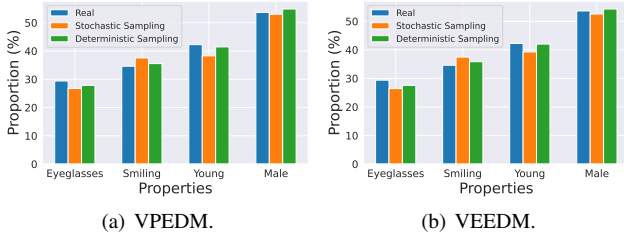


Figure 6: Attack performance on the EDM models.

Table 3: Quantitative attack results on the EDM models. Stoch.: Stochastic; Deter.: Deterministic.

Model	Sampler	FID	Property	Real Prop. (%)	Inferred Prop. (%)	Abs. Diff. (%)
VPEDM	Stoch.	2.87	Eyeglasses	29.39	26.73	2.66
			Smiling	34.61	37.54	2.93
			Young	42.25	38.28	3.97
			Male	53.62	53.01	0.61
	Deter.	2.47	Eyeglasses	29.39	27.83	1.56
			Smiling	34.61	35.54	0.93
			Young	42.25	41.44	0.81
			Male	53.62	54.85	1.23
VEEDM	Stoch.	2.85	Eyeglasses	29.39	26.44	2.95
			Smiling	34.61	37.47	2.86
			Young	42.25	39.27	2.98
			Male	53.62	52.55	1.07
	Deter.	2.57	Eyeglasses	29.39	27.54	1.85
			Smiling	34.61	35.85	1.24
			Young	42.25	42.02	0.23
			Male	53.62	54.3	0.68

we can observe that the inferred proportions of various private properties are all close to the real proportions. In addition, different types of sampling methods show similar high privacy risks in all properties and diffusion models.

Table 3 describes quantitative attack results on the EDM models. We can see that all samplers can achieve a good performance, obtaining an FID value between 2 and 3. We also report the absolute difference. The minimal absolute difference is 0.23%, which can be seen in inferring the property `young` on VEEDM using deterministic sampling. When inferring the property `young` in VPSDE under the stochastic sampling, our attack shows a little inferior performance with an absolute difference of 3.97%. To sum up, our attack on the EDM models can achieve at most a 4% absolute difference.

## 6 Defenses

In this section, we shift our focus to mitigating property inference attacks. We first discuss several potential defenses. Then we will introduce a property aware sampling method and present the defense results. Finally, we discuss the defense of diffusion models trained with differential privacy.

### 6.1 Key Idea of Defenses

Property inference attacks leverage generated samples from a diffusion model to estimate the proportions of the properties. To defend against this type of attack, model owners could manipulate the output of a diffusion model to disguise the real proportion of the property  $p_{s_i}$ .

In this work, we consider a binary sensitive property  $s_i$ , i.e.  $s_i = \{0, 1\}$  and  $p_{s_i} + \bar{p}_{s_i} = 1$ . The goal of our designed defenses is to make adversaries infer the proportion of a property  $\bar{p}_{s_i}$  as close as 0.5.<sup>4</sup> There are at least two reasons. Firstly, it can disguise the real proportion of the sensitive property. Secondly, because some properties, such as `gender`, are usually related to fairness, this choice can also ensure the fairness of a diffusion model.

### 6.2 Potential Defenses

Based on the key idea that the designed defenses make adversaries infer the proportion of a property as about 0.5, we discuss the following potential defenses.

**Dropping some samples of a larger proportion of the property.** If the real proportion of a property  $p_{s_i}$  is not equal to 0.5, model owners can choose to drop some generated samples of a larger proportion of the property to achieve a balance. To achieve this, model owners need property classifiers for protected sensitive properties and calculate the real-time statistics. In detail, model owners first collect all generated samples before releasing these samples. Then, model owners train a property inference classifier for each property. Finally, the trained classifier is used for predicting properties and some generated samples that have a high proportion of the properties will be dropped.

We assume there are  $n$  binary and independent sensitive properties. Furthermore, the proportion of the property  $s_i$  satisfies  $p_{s_i} + \bar{p}_{s_i} = 1$  and  $p_{s_i} \in (0, 0.5)$ , where  $p_{s_i}$  is the proportion containing this property and  $\bar{p}_{s_i}$  is the proportion not containing this property. In the worst case, the proportion of dropping samples is, at most  $1 - 2^n \prod_{i=1}^n p_{s_i}$ . For instance, considering that there is one sensitive property and its real proportion is 10%, i.e.  $p_{s_1} = 10\%$  and  $n = 1$ , then 80% samples among all generated samples will be discarded to achieve the balance, which is quite not economical. In particular, the sampling of diffusion models is time-consuming. For the number of sensitive properties more than one, the number of dropping samples is exponentially increasing. Therefore, this method is simple but not scalable.

**Using a balanced dataset for sensitive properties.** This method requires model owners to prepare a balanced dataset for sensitive properties, such as using a dataset containing 50% male samples for the property `gender`. Our extensive experiments in Section 4.4 show that this method indeed has

<sup>4</sup>This can also be a predefined value by the model provider.



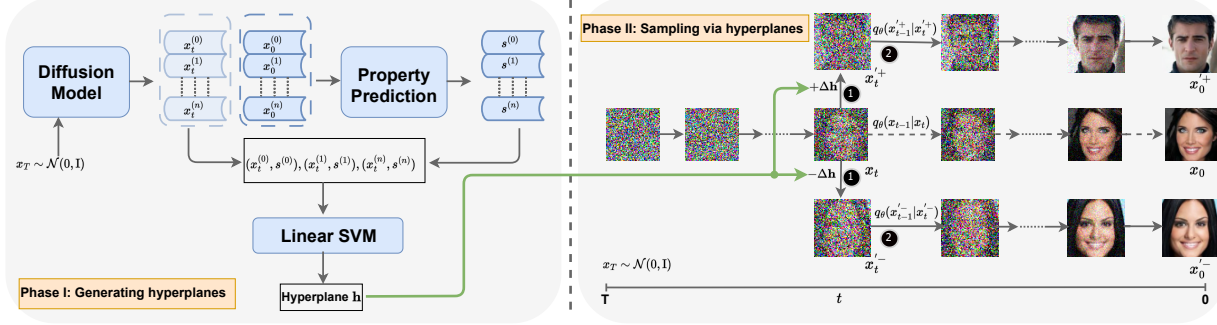


Figure 7: The process of the defense method PriSampler. Phase I learns hyperplanes of sensitive properties. Phase II synthesizes samples vis the learned hyperplanes. In ❶, at the  $t$  diffusion step, PriSampler changes the intermediate samples to the space of the specific sensitive property via the learned hyperplane. In ❷, PriSampler continues to denoise samples step by step. Eventually, the desired samples  $(x_0^{+}, x_0^{-})$  are obtained in the final step.

a positive effect to some degree. However, in some cases even for balanced properties, we also observe that the learned diffusion models will still produce imbalanced generated samples. For instance, the DPM sampler on the DDPM model trained on a 50% male dataset produces male samples which are about 46.37% of all generated samples. In addition, it is complicated to collect sufficient training samples if we need to consider balancing more sensitive properties.

**Property aware sampling.** In addition to above discussed methods, we can design a new type of sampling mechanism that can automatically balance the proportion of sensitive properties. In this way, we can avoid the waste of generated samples and fastidious dataset selection. We illustrate this method in the next subsection.

### 6.3 Defense Method — PriSampler

The main purpose of the property aware sampling method is to balance the proportion of sensitive properties in the sampling process of diffusion models. As a result, the inferred proportion always remains at about 0.5. Our method is inspired by the semantic latent space of generative adversarial network (GANs) in this work [36]. Due to the essential difference in the sampling process between diffusion models and GANs, we adapt the method to be well suitable for diffusion models and propose PriSampler as a general-purpose defense for diffusion models.

The key idea of PriSampler is to guild one sampler to generate novel samples in the latent space of sensitive properties. For instance, for the gender property, given the corresponding property hyperplane, samplers generate male samples on the side of this hyperplane and female samples on the opposite of this hyperplane. In order to find such a hyperplane, we use a linear support vector machine (SVM) to learn a decision boundary for each sensitive property. Then, given a base sampler, we directly use the boundary to guild the sampler to synthesize new samples. Here, the base sampler can be any

sampler that is used for sampling in prior work.

**The process of PriSampler.** Figure 7 shows the process of our defense — PriSampler. It consists of two phases: generating hyperplanes and sampling via hyperplanes. In phase I, our method aims to find a latent space in terms of a sensitive property from the diffusion model. To achieve this goal, we leverage a linear SVM to learn the hyperplane of the sensitive property. To be more specific, given a diffusion model, we can get many different types of generated samples from different diffusion steps. As shown in the left part of Figure 7, starting from Gaussian noise sample  $x_T \sim \mathcal{N}(0, I)$ , the diffusion model can produce the sample  $x_t$  at intermediate diffusion step  $t$  and the final sample  $x_0$  at the  $t = 0$  step. The final sample  $x_0$  is also the sample that we finally use. Then, the samples  $X_0 = \{x_0^{(0)}, x_0^{(1)}, \dots, x_0^{(n)}\}$  are inputted to a property prediction classifier and the corresponding prediction scores can be obtained, i.e.  $S = \{s^{(0)}, s^{(1)}, \dots, s^{(n)}\}$ . Instead of using  $X_0$ , we pair  $X_t$  and  $S$ . The data samples  $(X_t, S)$  will be used for training a linear SVM. A hyperplane corresponding to this property can be obtained from the well-trained SVM.

In phase II, our method aims to sample via the learned hyperplane. As shown in the right part of Figure 7, our method manipulate samples at the  $t$  diffusion step. To be specific, given Gaussian noise sample  $x_T \sim \mathcal{N}(0, I)$ , we can get the sample  $x_t$ . At the  $t$  diffusion step, we change the sampling direction via the learned hyperplane, and the samples with and without the corresponding sensitive property can be obtained. In the remaining diffusion step, the samples will continue to synthesize in the specific sensitive property latent space. Finally, samples with the balanced sensitive property can be generated. For different numbers of sensitive properties, the generated samples are calculated as follows.

**Single property.** Given a hyperplane  $\mathbf{h}$  obtained in phase I, and a sample  $x_t$  at step  $t$ , we can get  $x_t'$ :

$$x_t' = x_t + \alpha \mathbf{h}. \quad (4)$$

$\alpha$  is a hyperparameter, and we take a value  $\alpha > 0$  means that

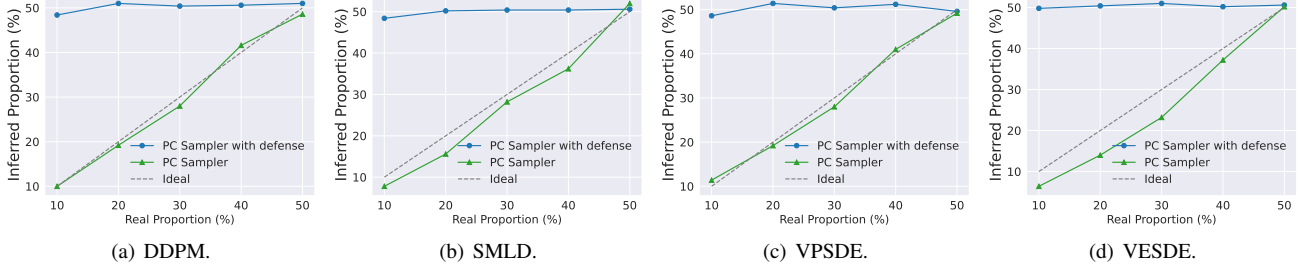


Figure 8: Defense performance on the PC sampler.

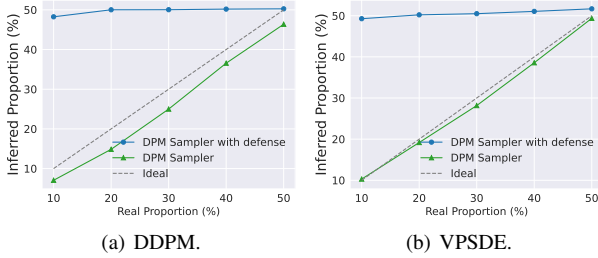


Figure 9: Defense performance on the DPM sampler.

a positive sample  $x_t^+$  is obtained and it has this property. A value  $\alpha < 0$  means a negative sample  $x_t^-$  is obtained and does not have this property. In this work, depending on different base samplers and diffusion models, we choose different  $\alpha$ . We provide the details in Appendix A.2.

**Multiple properties.** When there are multiple sensitive properties, the key idea is that we manipulate one property while keeping others unchanged. That is, we need to find a new hyperplane that is orthogonal to other hyperplanes. Take two properties as an example, we first manipulate the first one and manipulate the second condition on the first one. In this way, we can get generated samples with balanced properties. To be more specific, given two hyperplanes  $\mathbf{h}_1$  and  $\mathbf{h}_2$  obtained in phase I and a sample  $x_t$ . We first get a new hyperplane:

$$\mathbf{h}_2' = \mathbf{h}_1 - (\mathbf{h}_1^T \mathbf{h}_2) \mathbf{h}_2, \quad (5)$$

where  $(\mathbf{h}_1^T \mathbf{h}_2) \mathbf{h}_2$  is the projection of  $\mathbf{h}_1$  onto  $\mathbf{h}_2$ . The new hyperplane  $\mathbf{h}_2'$  equals the vector difference between  $\mathbf{h}_1$  and the projection of  $\mathbf{h}_1$  onto  $\mathbf{h}_2$ . Therefore,  $\mathbf{h}_2'$  is orthogonal to  $\mathbf{h}_1$ . Put another way,  $\mathbf{h}_2'$  can achieve that the second property is changed without impacting the first property. Then, based on Equation 4, we can get  $x_t'$  through  $x_t$  and  $\mathbf{h}_1$ . Given  $x_t'$  and  $\mathbf{h}_2'$ , we can obtain  $x_t''$ . Here, we require that the hyperplanes of multiple properties are independent, i.e. they are not in the same space. Otherwise, it is hard to find a hyperplane to guarantee that manipulating samples in this hyperplane does not affect the others. As introduced in Section 2.2, there are two types of samplings for diffusion models: stochastic sampling and deterministic sampling. Therefore, we implement our method on the PC sampler and the DPM sampler. We further provide the detailed algorithm in Appendix A.1.

## 6.4 Experimental Setup

We apply our method on two base samplers: one PC sampler for stochastic sampling and one DPM sampler for deterministic sampling. We directly use trained diffusion models from Section 4.3. In our defense, we use the library Sklearn to implement Linear SVM. We directly use trained property classifiers in Section 4.3 to predict scores  $S$ . We choose different diffusion steps for different samplers of diffusion models to manipulate. We summarize them in Appendix A.2. As discussed in Section 4.3, 500 generated samples for stochastic sampling and 50,000 generated samples for deterministic sampling are used for computing FID values.

## 6.5 Defense Results

**Defense performance on different samplers.** Figure 8 and Figure 9 present our defense performance to protect the sensitive property `male` for the PC sampler and the DPM sampler, respectively. Overall, our defense can achieve excellent performance. Even if the real proportion is 10%, our method can make adversaries get an inferred proportion of 50%.

Table 4 shows the corresponding quantitative results. Here, the absolute difference is the absolute difference between the inferred proportion  $\hat{p}_{s_i}$  and desired proportion  $\tilde{p}_{s_i}$ , i.e.  $|\hat{p}_{s_i} - \tilde{p}_{s_i}|$ . The best defense performance can be seen at SMLD trained on CelebA-50k-20% for the PC sampler and DDPM trained on CelebA-1k-20% for the DPM sampler. Their absolute differences are 0.2% and 0.02%, respectively. The worst defense performance is 1.6% for the PC sampler for DDPM trained on CelebA-1k-10%, and 1.68% for the DPM sampler for VPSDE trained on CelebA-1k-10%. Table 6 summarizes the results for each sampler among different diffusion models. For the single property `male`, the average absolute difference is 0.75% for the PC sampler and 0.64% for the DPM sampler. It indicates that our defense method can control the error of an inferred proportion below 1.00%.

**Defense performance on different diffusion models.** Figure 8 and Figure 9 present our defense performance on four types of diffusion models. Similarly, we can observe that the inferred proportions almost remain 50% for diffusion models trained on different datasets. It means our method can be

Table 4: Defense performances on a single property. Desi. Prop.: Desired Proportion.

Model	Real Prop. (%)	Desi. Prop. (%)	Inferred Prop. (%)	Abs. Diff. (%)	FID		Model	Real Prop. (%)	Desi. Prop. (%)	Inferred Prop. (%)	Abs. Diff. (%)	FID
PC Sampler												
DDPM	10	50	48.40	1.60	56.35	VPSDE	10	50	48.60	1.40	58.72	
	20	50	51.00	1.00	46.80		20	50	51.40	1.40	41.26	
	30	50	50.40	0.40	40.00		30	50	50.40	0.40	38.89	
	40	50	50.60	0.60	48.04		40	50	51.20	1.20	51.61	
	50	50	51.00	1.00	49.58		50	50	49.60	0.40	42.82	
SMLD	10	50	48.40	1.60	38.40	VESDE	10	50	49.80	0.20	61.32	
	20	50	50.20	0.20	44.68		20	50	50.40	0.40	68.95	
	30	50	50.40	0.40	45.52		30	50	51.00	1.00	57.47	
	40	50	50.40	0.40	45.17		40	50	50.20	0.20	77.57	
	50	50	50.60	0.60	46.95		50	50	50.60	0.60	49.75	
DPM Sampler												
DDPM	10	50	48.25	1.75	44.70	VPSDE	10	50	49.28	0.72	52.44	
	20	50	50.02	0.02	47.87		20	50	50.22	0.22	52.78	
	30	50	50.04	0.04	44.41		30	50	50.50	0.50	50.66	
	40	50	50.19	0.19	45.90		40	50	51.06	1.06	53.00	
	50	50	50.26	0.26	47.68		50	50	51.68	1.68	45.33	

Table 5: Defense performances on multiple properties.

Model		Real Prop. (%)	Desi. Prop. (%)	Inferred Prop. (%)	Abs. Diff. (%)		Real Prop. (%)	Desi. Prop. (%)	Inferred Prop. (%)	Abs. Diff. (%)	FID
PC sampler											
DDPM	Male	30	50	51.00	1.00	Young	79.40	50	57.40	7.40	48.74
VPSDE	Male	30	50	51.60	1.60	Young	79.40	50	54.20	4.20	45.95
DPM sampler											
DDPM	Male	30	50	50.53	0.53	Young	79.40	50	52.28	2.28	40.25
VPSDE	Male	30	50	52.73	2.73	Young	79.40	50	52.33	2.33	42.29

effectively applied to these different diffusion models.

**Defense performance on more than one property.** Figure 10 shows the defense performance to protect two sensitive properties male and young. Here, we choose the models trained on CelebA-1k-30% as target models. That is, the real proportion of the property male is 30%. The corresponding real proportion of the private property young is 79.4%. Overall, we can observe that the inferred proportions of both properties are about 50%, no matter the larger proportion or the smaller proportion.

Table 5 shows the corresponding quantitative results. Table 6 summarizes the result for male+young properties on both samplers. We can see that the average absolute difference is 3.55% for the PC sampler and 1.97% for the DPM sampler. We also note that the absolute difference on two properties is larger than that on the single property. One of the reasons is that these properties are entangled together in diffusion models. As a result, it might lead the hyperplane not to completely separate these properties. We will take this as our future work to design disentangled generative algorithms for diffusion models from the perspective of the training process to improve our defense performance on multiple properties.

**Defense performance on different numbers of generated samples.** Figure 11 shows the defense performance on different numbers of generated samples. Here, we choose the DDPM model trained on CelebA-1k-30% as the target model. The sensitive property is male. We can clearly see that both types of samplers can provide well protection for the property

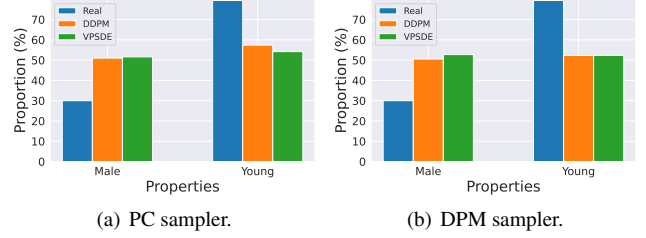


Figure 10: Defense performance for multiple properties.

Table 6: Summary of defense performances. Here, we report the average absolute difference (with standard deviation in parentheses) and the best and worst absolute difference.

Property	Sampler	Average (%)	Best (%)	Worst (%)
Male	PC	0.75 (0.48)	0.20	1.60
	DPM	0.64 (0.65)	0.02	1.75
Male+Young	PC	3.55 (2.92)	1.00	7.40
	DPM	1.97 (0.98)	0.53	2.73

male even if model owners only release only as few as 50 samples. Although the PC sampler shows a slight fluctuation in the phase of releasing a few samples, it is gradually stable after 500 samples. The DPM sampler extremely stabilizes no matter how many samples are released. One of the reason might be that random noise added during the sampling process for the PC sampler have some effects on generated samples because the PC sampler belongs to stochastic sampling while the DPM sampler belongs to deterministic sampling.

**Defense performance on different diffusion steps.** Figure 12 shows defense performance on different diffusion steps. Here, the target model is DDPM trained on CelebA-1k-30% and we use the PC sampler and the total number of sampling steps is 1,000, and the sensitive property is male. The blue line and the left axis show the inferred proportion while the red line and the right axis present the corresponding FID values. Generated samples in the 0 diffusion step are pure Gaussian noise while generated samples in the 999 step are realistic samples. Overall, we can see that defense performance and model utility in the latter stage of diffusion steps show better than that of the former stage. Generally, choosing late middle diffusion steps can obtain a good balance in defense performance, FID values, and the meaningfulness of generated images.

## 6.6 Comparison with Differential Privacy

Differential privacy [1, 10] is a common measure for defending against privacy attacks. In this subsection, we explore the feasibility of differential privacy to defend against property inference attacks. Furthermore, we make a comparison with our defense method PriSampler.

We use differentially private diffusion models (DPDMs) proposed by Dockhorn et. al [7], because they are the

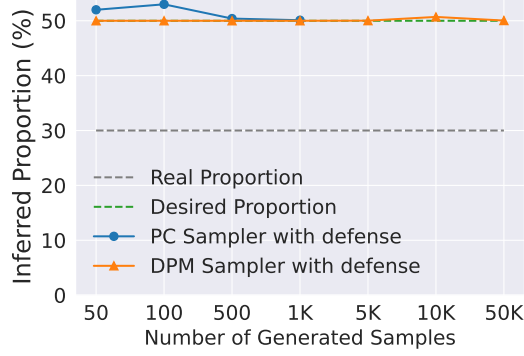


Figure 11: Performance on the number of generated samples.

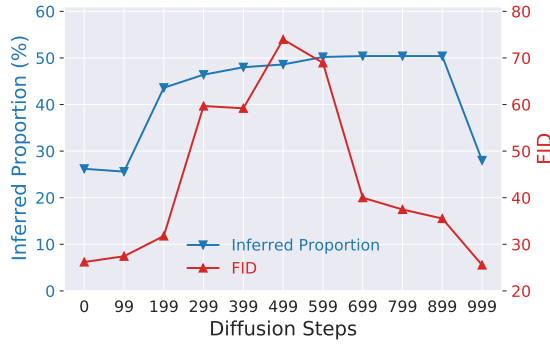


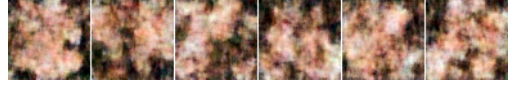
Figure 12: Defense performance on different diffusion steps.

first to apply differentially private stochastic gradient descent (DPSGD) [1] to diffusion models and can generate meaningful images. We adopt their suggested hyperparameters to train DPDMs. We set the number of epochs and batch sizes as 100, and 128 respectively. The image size is fixed at 64, and we choose different sizes of training sets, i.e. CelebA-1k-30% and CelebA-50k-30%, and different privacy budgets  $\epsilon$ , i.e.  $\epsilon = 10$  and  $\epsilon = 50$ . We fix  $\delta$  as  $10^{-6}$  for all models. Here, we synthesize samples by stochastic sampling because DPDMs [7] analyze that it can obtain better FID values under differential privacy conditions.

Table 7 presents the comparison between our method and DPDM. Figure 13 visually shows synthetic samples. For the CelebA-1k-30% dataset, DPDM almost can not generate meaningful images, which leads to an FID value of 446.35. In contrast, our method can achieve a 40.00 FID value and the inferred proportion is 50.50%. Figure 13(b) also shows the good quality of synthetic samples for our method PriSampler. For the CelebA-50k-30% dataset, we can clearly see that the generated samples from DPDM only have a vague shape of the human face. Even if we increase the privacy budget  $\epsilon$  from 10 to 50, the synthetic human face samples still are distorted, although we can see that FID decreases from 121.56 to 103.64. Here, note that  $\epsilon = 10$  is usually considered as low amounts of privacy. We also observe that the inferred proportion for DPDM under  $\epsilon = 10$  is 44.00%, while that for DPDM under  $\epsilon = 50$  is 24.20%. It indicates DPDM under smaller privacy budgets can disguise the real proportion of

Table 7: Comparison between PriSampler and DPDM. DDPM\* means PriSampler is applied to the DDPM model. SMLD\* means PriSampler is applied to the SMLD model.

	CelebA-1k-30%		CelebA-50k-30%		
	DPDM ( $\epsilon = 10$ )	DDPM*	DPDM ( $\epsilon = 10$ )	DPDM ( $\epsilon = 50$ )	SMLD*
FID	446.35	40.00	121.56	103.64	45.52
Inferred Prop.	100.00	50.40	44.00	24.20	50.40



(a)  $\epsilon = 10$ , DPDM trained on CelebA-1k-30%.



(b) PriSampler for DDPM trained on CelebA-1k-30%.



(c)  $\epsilon = 10$ , DPDM trained on CelebA-50k-30%.



(d)  $\epsilon = 50$ , DPDM trained on CelebA-50k-30%.



(e) PriSampler for SMLD trained on CelebA-50k-30%.

Figure 13: Visualization of synthetic samples under the defense DPDM and PriSampler.

certain properties to some extent. However, the quality of generated samples is too vague. In contrast, our method can still synthesize meaningful samples with a balanced proportion.

## 7 Discussion

Our method PriSampler aims to navigate a sampler in the property space and is operated in the sampling process. Thus, it is a training-free method. Furthermore, it is a model-agnostic and can be used as a plug-in for a wide range of diffusion models. In this section, we discuss limitations and future work.

**Model utility.** Although our method PriSampler can guarantee the defense performance, i.e. achieving the desired proportions that model owners wish, it will sacrifice model utility to some extent. Nevertheless, we take the first step to protect diffusion models from property inference attacks. Furthermore, our defense method is still promising and competitive, compared to diffusion models trained with differential privacy.

**Non-binary property.** Our defense method PriSampler in



this work mainly considers binary property which has two values. For instance, the value of the binary property `gender` has 0 (male) and 1 (female). When the property is non-binary, i.e. the value of a property has multiple categories or is continuous, our method PriSampler can also be applied by transforming this property as a binary property.

**Entangled properties.** We observe that when our defense method is applied to protect multiple sensitive properties, the defense performance, i.e. the average absolute difference, becomes slightly worse, compared to that applied to the single property. This might be because these properties are entangled together due to the training mechanism of existing diffusion models. As a result, it is difficult to find an ideal hyperplane to completely differentiate them. In the future, we intend to design diffusion models with disentangled properties, which aim to separate entangled properties as large as possible in the training process. In that way, our defense method can further improve the protection performance for diffusion models.

**Membership inference.** Membership inference and property inference are two main types of privacy attacks, but their attack goals are different. Membership inference involves the privacy of individual training sample of a training set while property inference involves the privacy of global properties of a training set. In the future, we plan to study the relationship between two types of privacy attacks and provide a holistic defense measure.

**Attacks via weights.** Our attack method only utilizes the synthetic data from a diffusion model to mount property inference attacks. Prior work on classification models [11] has proposed to infer the sensitive properties by the weights of a full-connected neural network. Therefore, we plan to investigate the feasibility of property inference attacks by utilizing the weights of diffusion models themselves.

## 8 Related Work

**Diffusion models.** Diffusion models [14, 38] have recently drawn immense attention to academia and industry due to their high success in synthesizing realistic images. Subsequently, various methods [18, 26, 26, 39–41] are proposed to further improve the performance of diffusion models from the perspective of the training process, sampling mechanisms. Beyond image synthesis, they have been applied to a variety of novel applications, such as image restoration [34, 43], super-resolution [15, 35]. However, these works focus on improving the generative performance of diffusion models. In this work, considering the increasing popularity of diffusion models, we study diffusion models from the viewpoint of privacy.

**Property inference attacks.** Property inference attacks allow adversaries to infer global sensitive information of the training set from a machine learning model. They are firstly studied by Ateniese et al. [3] on simple machine learning models, such as SVM and Hidden Markov Models. Since then, there are a

more increasing number of works focusing on property inference in neural network models, such as fully-connected neural networks [11], convolution neural networks [5, 27, 42], generative adversarial networks [48], graph neural networks [47], and federated learning models [29]. However, these works mainly focus on attacks, and their attack methods heavily rely on shadow models which require a large amount of computation. Furthermore, property inference attacks on emerging diffusion models have not yet been extensively studied. In this work, we take the first step to explore property inference attacks against various types of diffusion models under more realistic attack scenarios and affordable attack costs: the adversaries perform the inference only utilizing synthetic data. More importantly, we propose a set of effective defense measures to safeguard sensitive properties of diffusion models.

There are several works studying privacy attacks against diffusion models through the lens of membership inference attacks [4, 9, 17, 28, 44, 49]. However, membership inference attacks aim to infer whether a sample was used for training a machine learning model and focus more on the privacy of the individual training sample of the training set. In contrast, this work endeavors to study property inference attacks which aim to infer the globally sensitive information of the training set used for diffusion models.

## 9 Conclusion

In this paper, we have presented the first study about property inference of diffusion models. Under the property inference attack which only utilizes the synthetic data, we have investigated the property inference risks on four different types of diffusion models and two different types of sampling mechanisms (in total twenty diffusion models and three samplers). Our extensive empirical analysis has shown that various diffusion models and their samplers are vulnerable to property inference attacks. For instance, as few as 500 generated samples can precisely infer the real proportion of a property. More severely, better performance of diffusion models can lead to a more accurate estimation of property inference, which indicates that we should consider privacy concerns when consistently pursuing the generation performance of a diffusion model. We have also shown the property inference attack is still effective at inferring off-the-shelf pre-trained diffusion models in reality. We also developed a model-agnostic plug-in defense method PriSampler and demonstrated its effectiveness with various different types of samplers and diffusion models. Our PriSampler further shows significant performance in model utility and defense performance, when compared with diffusion models trained with differential privacy.

We have also identified several directions for future work, including developing attack methods via weights, designing diffusion models with disentangled properties, and constructing a holistic defense method by exploring the relationship between property inference and membership inference.

## Acknowledgments

This research was funded in whole by the Luxembourg National Research Fund (FNR), grant reference 13550291.

## References

- [1] Martin Abadi, Andy Chu, Ian Goodfellow, H Brendan McMahan, Ilya Mironov, Kunal Talwar, and Li Zhang. Deep learning with differential privacy. In *Proceedings of ACM SIGSAC Conference on Computer and Communications Security (CCS)*, pages 308–318. ACM, 2016.
- [2] Brian DO Anderson. Reverse-time diffusion equation models. *Stochastic Processes and their Applications*, 12(3):313–326, 1982.
- [3] Giuseppe Ateniese, Luigi V Mancini, Angelo Spognardi, Antonio Villani, Domenico Vitali, and Giovanni Felici. Hacking smart machines with smarter ones: How to extract meaningful data from machine learning classifiers. *International Journal of Security and Networks*, 10(3):137–150, 2015.
- [4] Nicholas Carlini, Jamie Hayes, Milad Nasr, Matthew Jagielski, Vikash Sehwal, Florian Tramèr, Borja Balle, Daphne Ippolito, and Eric Wallace. Extracting training data from diffusion models. *arXiv preprint arXiv:2301.13188*, 2023.
- [5] Harsh Chaudhari, John Abascal, Alina Oprea, Matthew Jagielski, Florian Tramèr, and Jonathan Ullman. Snap: Efficient extraction of private properties with poisoning. In *Proceedings of IEEE Symposium on Security and Privacy (SP)*, pages 1935–1952. IEEE, 2023.
- [6] Prafulla Dhariwal and Alexander Nichol. Diffusion models beat gans on image synthesis. In *Proceedings of Annual Conference on Neural Information Processing Systems (NeurIPS)*, pages 8780–8794. Curran Associates, Inc., 2021.
- [7] Tim Dockhorn, Tianshi Cao, Arash Vahdat, and Karsten Kreis. Differentially private diffusion models. *arXiv preprint arXiv:2210.09929*, 2022.
- [8] John R Dormand and Peter J Prince. A family of embedded runge-kutta formulae. *Journal of Computational and Applied Mathematics*, 6(1):19–26, 1980.
- [9] Jinhao Duan, Fei Kong, Shiqi Wang, Xiaoshuang Shi, and Kaidi Xu. Are diffusion models vulnerable to membership inference attacks? *arXiv preprint arXiv:2302.01316*, 2023.
- [10] Cynthia Dwork. Differential privacy: A survey of results. In *Proceedings of International Conference on Theory and Applications of Models of Computation (TAMC)*, volume 4978 of *Lecture Notes in Computer Science*, pages 1–19. Springer, 2008.
- [11] Karan Ganju, Qi Wang, Wei Yang, Carl A Gunter, and Nikita Borisov. Property inference attacks on fully connected neural networks using permutation invariant representations. In *Proceedings of ACM SIGSAC Conference on Computer and Communications Security (CCS)*, pages 619–633. ACM, 2018.
- [12] Shansan Gong, Mukai Li, Jiangtao Feng, Zhiyong Wu, and Lingpeng Kong. Sequence to sequence text generation with diffusion models. In *Proceedings of International Conference on Learning Representations (ICLR)*, 2023.
- [13] Ian Goodfellow, Jean Pouget-Abadie, Mehdi Mirza, Bing Xu, David Warde-Farley, Sherjil Ozair, Aaron Courville, and Yoshua Bengio. Generative adversarial nets. In *Proceedings of Annual Conference on Neural Information Processing Systems (NeurIPS)*, pages 2672–2680. Curran Associates, Inc., 2014.
- [14] Jonathan Ho, Ajay Jain, and Pieter Abbeel. Denoising diffusion probabilistic models. In *Proceedings of Annual Conference on Neural Information Processing Systems (NeurIPS)*, volume 33, pages 6840–6851. Curran Associates, Inc., 2020.
- [15] Jonathan Ho, Chitwan Saharia, William Chan, David J Fleet, Mohammad Norouzi, and Tim Salimans. Cascaded diffusion models for high fidelity image generation. *Journal of Machine Learning Research*, 23(47):1–33, 2022.
- [16] Jonathan Ho, Tim Salimans, Alexey A Gritsenko, William Chan, Mohammad Norouzi, and David J Fleet. Video diffusion models. In *ICLR Workshop on Deep Generative Models for Highly Structured Data*, 2022.
- [17] Hailong Hu and Jun Pang. Membership inference of diffusion models. *arXiv preprint arXiv:2301.09956*, 2023.
- [18] Tero Karras, Miika Aittala, Timo Aila, and Samuli Laine. Elucidating the design space of diffusion-based generative models. In *Proceedings of Annual Conference on Neural Information Processing Systems (NeurIPS)*. Curran Associates, Inc., 2022.
- [19] Tero Karras, Samuli Laine, and Timo Aila. A style-based generator architecture for generative adversarial networks. In *Proceedings of IEEE/CVF Conference on Computer Vision and Pattern Recognition (CVPR)*, pages 4401–4410. IEEE, 2019.

- [20] Amirhossein Kazerooni, Ehsan Khodapanah Aghdam, Moein Heidari, Reza Azad, Mohsen Fayyaz, Ilker Hacıhaliloglu, and Dorit Merhof. Diffusion models for medical image analysis: A comprehensive survey. *arXiv preprint arXiv:2211.07804*, 2022.
- [21] Diederik P Kingma and Max Welling. Auto-encoding variational bayes. In *Proceedings of International Conference on Learning Representations (ICLR)*, 2014.
- [22] Zhifeng Kong, Wei Ping, Jiaji Huang, Kexin Zhao, and Bryan Catanzaro. Diffwave: A versatile diffusion model for audio synthesis. In *Proceedings of International Conference on Learning Representations (ICLR)*, 2021.
- [23] Xiang Li, John Thickstun, Ishaan Gulrajani, Percy S Liang, and Tatsunori B Hashimoto. Diffusion-lm improves controllable text generation. In *Proceedings of Annual Conference on Neural Information Processing Systems (NeurIPS)*, volume 35, pages 4328–4343. Curran Associates, Inc., 2022.
- [24] Luping Liu, Yi Ren, Zhijie Lin, and Zhou Zhao. Pseudo numerical methods for diffusion models on manifolds. In *Proceedings of International Conference on Learning Representations (ICLR)*, 2022.
- [25] Ziwei Liu, Ping Luo, Xiaogang Wang, and Xiaoou Tang. Deep learning face attributes in the wild. In *Proceedings of IEEE International Conference on Computer Vision (ICCV)*, pages 3730–3738. IEEE, 2015.
- [26] Cheng Lu, Yuhao Zhou, Fan Bao, Jianfei Chen, Chongxuan Li, and Jun Zhu. Dpm-solver: A fast ode solver for diffusion probabilistic model sampling in around 10 steps. In *Proceedings of Annual Conference on Neural Information Processing Systems (NeurIPS)*. Curran Associates, Inc., 2022.
- [27] Saeed Mahloujifar, Esha Ghosh, and Melissa Chase. Property inference from poisoning. In *Proceedings of IEEE Symposium on Security and Privacy (SP)*, pages 1569–1569. IEEE, 2022.
- [28] Tomoya Matsumoto, Takayuki Miura, and Naoto Yanai. Membership inference attacks against diffusion models. *arXiv preprint arXiv:2302.03262*, 2023.
- [29] Luca Melis, Congzheng Song, Emiliano De Cristofaro, and Vitaly Shmatikov. Exploiting unintended feature leakage in collaborative learning. In *Proceedings of IEEE Symposium on Security and Privacy (SP)*, pages 691–706. IEEE, 2019.
- [30] Alex Nichol, Prafulla Dhariwal, Aditya Ramesh, Pranav Shyam, Pamela Mishkin, Bob McGrew, Ilya Sutskever, and Mark Chen. Glide: Towards photorealistic image generation and editing with text-guided diffusion models. *arXiv preprint arXiv:2112.10741*, 2021.
- [31] Eckhard Platen and Nicola Bruti-Liberati. *Numerical solution of stochastic differential equations with jumps in finance*, volume 64. Springer Science & Business Media, 2010.
- [32] Aditya Ramesh, Prafulla Dhariwal, Alex Nichol, Casey Chu, and Mark Chen. Hierarchical text-conditional image generation with clip latents. *arXiv preprint arXiv:2204.06125*, 2022.
- [33] Olga Russakovsky, Jia Deng, Hao Su, Jonathan Krause, Sanjeev Satheesh, Sean Ma, Zhiheng Huang, Andrej Karpathy, Aditya Khosla, Michael Bernstein, Alexander C. Berg, and Li Fei-Fei. Imagenet large scale visual recognition challenge. *International Journal of Computer Vision*, 115(3):211–252, 2015.
- [34] Chitwan Saharia, William Chan, Huiwen Chang, Chris Lee, Jonathan Ho, Tim Salimans, David Fleet, and Mohammad Norouzi. Palette: Image-to-image diffusion models. In *Proceedings of ACM International Conference on Computer Graphics and Interactive Techniques (SIGGRAPH)*, pages 1–10. ACM, 2022.
- [35] Chitwan Saharia, Jonathan Ho, William Chan, Tim Salimans, David J Fleet, and Mohammad Norouzi. Image super-resolution via iterative refinement. *IEEE Transactions on Pattern Analysis and Machine Intelligence*, 45(4):4713–4726, 2023.
- [36] Yujun Shen, Jinjin Gu, Xiaoou Tang, and Bolei Zhou. Interpreting the latent space of gans for semantic face editing. In *Proceedings of IEEE/CVF Conference on Computer Vision and Pattern Recognition (CVPR)*, pages 9243–9252. IEEE, 2020.
- [37] Reza Shokri, Marco Stronati, Congzheng Song, and Vitaly Shmatikov. Membership inference attacks against machine learning models. In *Proceedings of IEEE Symposium on Security and Privacy (SP)*, pages 3–18. IEEE, 2017.
- [38] Jascha Sohl-Dickstein, Eric Weiss, Niru Maheswaranathan, and Surya Ganguli. Deep unsupervised learning using nonequilibrium thermodynamics. In *Proceedings of International Conference on Machine Learning (ICML)*, pages 2256–2265. PMLR, 2015.
- [39] Jiaming Song, Chenlin Meng, and Stefano Ermon. Denoising diffusion implicit models. In *Proceedings of International Conference on Learning Representations (ICLR)*, 2021.
- [40] Yang Song and Stefano Ermon. Generative modeling by estimating gradients of the data distribution. In *Proceedings of Annual Conference on Neural Information Processing Systems (NeurIPS)*, volume 32. Curran Associates, Inc., 2019.

- [41] Yang Song, Jascha Sohl-Dickstein, Diederik P Kingma, Abhishek Kumar, Stefano Ermon, and Ben Poole. Score-based generative modeling through stochastic differential equations. In *Proceedings of International Conference on Learning Representations (ICLR)*, 2021.
- [42] Anshuman Suri and David Evans. Formalizing and estimating distribution inference risks. *Proceedings on Privacy Enhancing Technologies*, 4:528–551, 2022.
- [43] Yinhuai Wang, Jiwen Yu, and Jian Zhang. Zero-shot image restoration using denoising diffusion null-space model. *arXiv preprint arXiv:2212.00490*, 2022.
- [44] Yixin Wu, Ning Yu, Zheng Li, Michael Backes, and Yang Zhang. Membership inference attacks against text-to-image generation models. *arXiv preprint arXiv:2210.00968*, 2022.
- [45] Ling Yang, Zhilong Zhang, Yang Song, Shenda Hong, Runsheng Xu, Yue Zhao, Yingxia Shao, Wentao Zhang, Bin Cui, and Ming-Hsuan Yang. Diffusion models: A comprehensive survey of methods and applications. *arXiv preprint arXiv:2209.00796*, 2022.
- [46] Qingsheng Zhang and Yongxin Chen. Fast sampling of diffusion models with exponential integrator. In *Proceedings of International Conference on Learning Representations (ICLR)*, 2023.
- [47] Zhikun Zhang, Min Chen, Michael Backes, Yun Shen, and Yang Zhang. Inference attacks against graph neural networks. In *Proceedings of USENIX Security Symposium (USENIX Security)*, pages 4543–4560. USENIX Association, 2022.
- [48] Junhao Zhou, Yufei Chen, Chao Shen, and Yang Zhang. Property inference attacks against GANs. In *Proceedings of Network and Distributed Systems Security Symposium (NDSS)*. Internet Society, 2022.
- [49] Derui Zhu, Dingfan Chen, Jens Grossklags, and Mario Fritz. Data forensics in diffusion models: A systematic analysis of membership privacy. *arXiv preprint arXiv:2302.07801*, 2023.

## A Appendix

### A.1 Implementation Details of PriSampler

In this section, we detail our defense method PriSampler. Specifically, in Algorithm 1, the function `GeneratingHyperplanes` is utilized to learn the hyperplanes of properties from a given diffusion model, which corresponds to Phase I of Figure 7, while the function `sampling` is utilized to synthesize new samples in the learned hyperplanes, which corresponds to Phase II of Figure 7. For

---

### Algorithm 1: The PriSampler Algorithm

---

**Input:** a frozen pre-trained diffusion model:  $\mathcal{G}_\theta$ ; a base sampler:  $q_\theta(x_{t-1}|x_t)$ ; the trained property classifier of the private property  $s_i$ :  $\mathcal{P}_{s_i}$ ; the number of generated samples:  $m$ ; the number of hyperplanes:  $k$ ;

**Output:** Generated samples:  $X_{gen}$

```

1 def generatingHyperplanes( $\mathcal{G}_\theta, \mathcal{P}_{s_i}, q_\theta, k$ ):
2    $H = []$ ;
3   for  $i = 1$  to  $k$  do
4     Sample  $n$  samples  $X$  and  $n$  intermediate samples  $X_t$ 
       from  $\mathcal{G}_\theta$  using a base sampler  $q_\theta(x_{t-1}|x_t)$ ;
5      $S \leftarrow \mathcal{P}_{s_i}(X)$ ;  $\triangleright$  get prediction scores.
6      $\mathcal{L} \leftarrow \text{trainLinearSVM}(X_t, S)$ ;
7      $\mathbf{h} \leftarrow \text{getHyperplanes}(\mathcal{L})$ ;
8      $H.append(\mathbf{h})$ ;
9   return  $H$ 

10 def sampling( $H, m, q_\theta$ ):
11    $X_{gen} = []$ ;
12   while  $i < \lceil \frac{m}{k+1} \rceil$  do
13     initial sample  $x_T \sim \mathcal{N}(0, I)$ ;
14     if  $k == 1$  then
15        $X_{gen}.append(\text{samplingSingle}(H, q_\theta, x_T))$ ;
          $\triangleright$  For single property.
16     if  $k > 1$  then
17        $X_{gen}.append(\text{samplingMulti}(H, q_\theta, x_T))$ ;
          $\triangleright$  For multiple properties.
18   return  $X_{gen}$ 

19  $H \leftarrow \text{generatingHyperplanes}(\mathcal{G}_\theta, \mathcal{P}_{s_i}, q_\theta, k)$ ;
20  $X_{gen} \leftarrow \text{sampling}(H, m, q_\theta)$ ;
21 return  $X_{gen}$ 

```

---

a single property, we use the function `samplingSingle` to synthesize samples while the function `samplingMulti` is used to generate samples for the cases of multiple properties.

In our defense, we consider two types of sampling: stochastic sampling — the PC sampler, and deterministic sampling — the DPM sampler. Therefore, the base sampler  $q_\theta(x_{t-1}|x_t)$  of Algorithm 1 in the concrete implementation is the PC sampler and the DPM sampler, respectively. Note that the PC sampler consists of a predictor and a correcter in their original paper [41]. We only use the predictor of the PC sampler when  $i \leq t$ , in order to avoid the change of the sampling direction by the correcter.

### A.2 Hyperparameters of PriSampler

As introduced in Section 6.3, our method PriSampler has two hyperparameters:  $\alpha$  and  $t$ .  $\alpha$  controls the distance of the desired samples  $x'_t$  from an intermediate sample  $x_t$ .  $t$  is the diffusion step in which we manipulate an intermediate sample in the  $t$  step. Table 8 shows the hyperparameters  $\alpha$  and  $t$  used for different samplers and diffusion models. For base samplers, the total number of sampling steps is 40 for the DPM sampler and 1,000 for the PC sampler. In terms of the



Table 8: Hyperparameters ( $\alpha, t$ ) of PriSampler for different samplers and diffusion models.

Sampler	Model	CelebA-1k-10		CelebA-1k-20		CelebA-1k-30		CelebA-1k-40		CelebA-1k-50	
		$\alpha$	$t$	$\alpha$	$t$	$\alpha$	$t$	$\alpha$	$t$	$\alpha$	$t$
PC	DDPM	150	699	150	699	150	699	140	699	140	699
	VPSDE	220	699	150	699	170	699	150	699	140	699
DPM	DDPM	50	6	50	6	50	6	50	6	50	6
	VPSDE	50	6	50	6	50	6	50	6	50	6
Sampler	Model	CelebA-50k-10		CelebA-50k-20		CelebA-50k-30		CelebA-50k-40		CelebA-50k-50	
		$\alpha$	$t$	$\alpha$	$t$	$\alpha$	$t$	$\alpha$	$t$	$\alpha$	$t$
PC	SMLD	40	500	40	500	40	500	40	500	40	500
	VESDE	25	549	25	549	25	549	15	549	10	549

Algorithm 2: The samplingSingle Algorithm

```

1 def samplingSingle( $H, q_\theta, x_T$ ):
2   for  $i = T - 1$  to 0 do
3     if  $i > t$  then
4        $x_{i-1} \leftarrow q_\theta(x_{i-1}|x_i)$ ;
5       ▷ Denoise when  $i > t$ .
6     if  $i == t$  then
7        $x_i^+, x_i^- \leftarrow \text{getSamples}(H[0], x_i)$ ;
8       ▷ At the  $t$  step, get samples in the corresponding
9         hyperplane by Equation 4.
10    if  $i \leq t$  then
11      ▷ Continue denoising when  $i \leq t$ .
12       $x_{i-1}^+ \leftarrow q_\theta(x_{i-1}^+|x_i^+)$ ;
13       $x_{i-1}^- \leftarrow q_\theta(x_{i-1}^-|x_i^-)$ ;
14  return  $x_0^+, x_0^-$ 

```

Algorithm 3: The samplingMulti Algorithm

```

1 def samplingMulti( $H, q_\theta, x_T$ ):
2   for  $i = T - 1$  to 0 do
3     if  $i > t$  then
4        $x_{i-1} \leftarrow q_\theta(x_{i-1}|x_i)$ ;
5     if  $i == t$  then
6        $x_i^+, x_i^- \leftarrow \text{getSamples}(H[0], x_i)$ ;
7       ▷ get samples in the  $H[0]$  by Equation 4.
8        $h_2' \leftarrow \text{getCondHyper}(H[0], H[1])$ ;
9       ▷ get a new hyperplane by Equation 5.
10       $x_i^{++}, x_i^{+-} \leftarrow \text{getSamples}(h_2', x_i^+)$ ;
11      ▷ get samples in the  $h_2'$  by Equation 4.
12       $x_i^{-+}, x_i^{--} \leftarrow \text{getSamples}(h_2', x_i^-)$ ;
13      ▷ get samples in the  $h_2'$  by Equation 4.
14    if  $i \leq t$  then
15       $x_{i-1}^{++} \leftarrow q_\theta(x_{i-1}^{++}|x_i^{++})$ ;
16       $x_{i-1}^{+-} \leftarrow q_\theta(x_{i-1}^{+-}|x_i^{+-})$ ;
17       $x_{i-1}^{-+} \leftarrow q_\theta(x_{i-1}^{-+}|x_i^{-+})$ ;
18       $x_{i-1}^{--} \leftarrow q_\theta(x_{i-1}^{--}|x_i^{--})$ ;
19  return  $x_0^{++}, x_0^{+-}, x_0^{-+}, x_0^{--}$ 

```

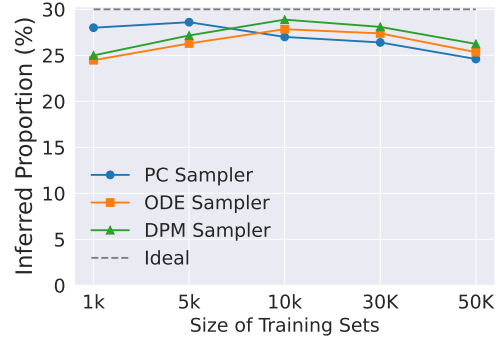


Figure 14: Attack performance with respect to different sizes of training sets. The target models are DDPM models trained on CelebA with the property male of 30%.

base sampler — DPM sampler, we set its hyperparameter ‘dpm\_solver\_method’ as ‘singlestep’, and ‘dpm\_solver\_order’ as ‘3’. Therefore, for PriSampler applied to the DPM sampler, we set  $\alpha$  and  $t$  as 50 and 6. Note, here,  $t = 6$  is the index of diffusion steps rather than actual diffusion steps, because the step size of the DPM sampler is equal to 3, i.e. ‘dpm\_solver\_order’ = ‘3’. In terms of the base sampler — PC sampler, we set its hyperparameter ‘predictor’ as ‘ReverseDiffusionPredictor’, and ‘corrector’ as ‘LangevinCorrector’. For PriSampler applied to the PC sampler, we choose different  $\alpha$  and  $t$  for different diffusion models, as shown in Table 8. This is because the PC sampler is stochastic sampling where fresh noise will be added in the sampling process, which may affect the generated samples in the protected property space. Therefore, we adjust  $\alpha$  and  $t$  to achieve the desired proportion.

### A.3 Additional Results

**Attack performance on different sizes of training sets.** Figure 14 plots attack performance in terms of sizes of training sets. Here, the target models are the DDPM models trained on a dataset containing 30% male training samples. Therefore, the real proportion of the property male is 30%. We can see that the inference performance slightly decreases with the increase in the size of training sets. For example, for the DPM sampler, when the size of training sets increases from 10k to 50k, the inferred proportions decrease from about 29% to around 26%. Overall, the inferred proportions for all samplers fluctuate between 25% and 30%.